Journal of Controlled Release 147 (2010) 368–376

Contents lists available at ScienceDirect

Journal of Controlled Release

journal homepage: www.elsevier.com/locate/jconrel

Sunlight triggered photodynamic ultradeformable liposomes against *Leishmania braziliensis* are also leishmanicidal in the dark

Jorge Montanari [a], Cristina Maidana [b], Mónica Inés Esteva [b], Cristina Salomon [c], Maria Jose Morilla [a], Eder L. Romero [a,*]

[a] Programa de Nanomedicinas, Departamento de Ciencia y Tecnología, Universidad Nacional de Quilmes, Roque Saenz Peña 352, Bernal, B1876 BXD, Buenos Aires, Argentina
[b] Instituto Nacional de Parasitologia Dr. Mario Fatala Chaben, Paseo Colon 568, 1063, Buenos Aires, Argentina
[c] Área Microbiología, Facultad de Ciencias Médicas, Universidad Nacional de Cuyo. Av. Libertador 80. Centro Universitario, 5500, Mendoza. Argentina

ARTICLE INFO

Article history:
Received 15 June 2010
Accepted 11 August 2010
Available online 19 August 2010

Keywords:
Ultradeformable liposomes
Cutaneous leishmaniasis
Photodynamic therapy
Transcutaneous

ABSTRACT

Being independent of artificial power sources, self administered sunlight triggered photodynamic therapy could be a suitable alternative treatment for cutaneous leishmaniasis, that avoids the need for injectables and the toxic side effects of pentavalent antimonials. In this work we have determined the *in vitro* leishmanicidal activity of sunlight triggered photodynamic ultradeformable liposomes (UDL). ZnPc is a hydrophobic Zn phthalocyanine that showed 20% anti-promastigote activity (APA) and 20% anti-amastigote activity (AA) against *Leishmania braziliensis* (strain 2903) after 15 min sunlight irradiation (15 J/cm^2). However, when loaded in UDL as UDL-ZnPc (1.25 μM ZnPc–1 mM phospholipids) it elicited 100% APA and 80% AA at the same light dose. In the absence of host cell toxicity, UDL and UDL-ZnPc also showed non-photodynamic leishmanicidal activity. Confocal laser scanning microscopy of cryosectioned human skin mounted in non-occlusive Saarbrücken Penetration Model, showed that upon transcutaneous administration ZnPc penetrated nearly 10 folds deeper as UDL-ZnPc than if loaded in conventional liposomes (L-ZnPc). Quantitative determination of ZnPc confirmed that UDL-ZnPc penetrated homogeneously in the *stratum corneum*, carrying 7 folds higher amount of ZnPc 8 folds deeper than L-ZnPc. It is envisioned that the multiple leishmanicidal effects of UDL-ZnPc could play a synergistic role in prophylaxis or therapeutic at early stages of the infection.

1. Introduction

Cutaneous (CL) and mucocutaneous leishmaniasis (MCL) are clinical manifestations of a group of diseases caused by dimorphic protozoa that belong to different species of the *Leishmania genus*, [1] which are transmitted to humans by sandfly bites. Infective parasites are hosted in skin macrophages and produce ulcerative lesions [2] as well as destructive mucosa inflammation in MCL [3]. 1.5 million new cases of CL arise worldwide each year [4], presenting a complex epidemiology that depends on intra and inter species variations [5]. The CL's geographic incidence is heterogeneous, including densely affected foci and dissemination areas in constant change [6] due to emigrations, tourism [7,8], urbanization [9] and the expansion of suitable ecosystems for the vector due to climatic changes [10]. A marked increase of cases in Europe and America has been recorded in the last decades, and new important epidemic foci have emerged [4,11].

Standard treatments are based on systemic or intralesional administration of pentavalent antimonials according to the leishmania specie and the clinical symptoms (intravenous or intramuscular 20–50 mg Sb(v)/kg weight/day for 30 days, or 1–3 ml under the edge of lesion and entire lesion every 5–7 days for a total of 2–5 times [12]), systemic amphotericin B or pentamidine isothionate [13,14]. The response to the treatment is slow and even inefficacious according to the species, with incomplete cure and relapse occurring within 6 months [13]. Treatments are linked to side effects such as hepatic alterations, biochemical pancreatitis, flattening of T waves in ECG, myalgia, arthralgia, thrombocytopenia, transient suppression of bone marrow and reversible renal insufficiency [15].

Thus, the search for an effective, simple, and low-cost treatment for CL that can be conveniently administered is still an active topic. In this scenario, topical treatment is preferable to systemic interventions [16]. The ointment of the highly hydrophilic antibiotic paromomycin (15%) associated to the permeation enhancer methyl benzethonium chloride (12%) (MBC), is relatively effective for CL treatment (*L. major*, *L. tropica*, *L. mexicana and L. panamensis*), but local side effects are frequently observed due to MBC [17]. On the other hand, topical amphotericin B (Amphocil in 5% ethanol) has been successful in treatment of *L. major* infected patients in Israel [18,19], but the high cost of Amphocil restricts their use and more extensive studies are needed.

* Corresponding author. Tel.: +54 1143657100; fax: +54 1143657132.
E-mail address: elromero@unq.edu.ar (E.L. Romero).

0168-3659/$ – see front matter © 2010 Elsevier B.V. All rights reserved.
doi:10.1016/j.jconrel.2010.08.014

Photodynamic therapy (PDT) is a potentially applicable, safe and affordable technology that is currently in use for the treatment of cancer and age-related macular degeneration. PDT is based on the concept that a photoactivatable compound, called a photosensitizer, can be excited by light of the appropriate wavelength to generate cytotoxic singlet oxygen and free radicals [20]. PDT is an attractive option to conventional antimicrobial chemotherapy, since it does not induce resistant strains neither upon multiple treatments [21,22]. Although PDT has rendered several cases of cure with good cosmetic results [23,24], the lack of standarized data and the need for special medical equipment (lamps), have hampered the use of PDT against CL [25]. The use of daylight to PDT can be an alternative to this last drawback. Recently a Phase II clinical trial in Israel has been started to determine the efficiency of methyl aminolevulinate (MAL)-PDT daylight triggered for the treatment of CL (*L. major* and *L. tropica*) [26].

In the present work, we have determined the *in vitro* leishmanicidal activity of the hydrophobic photosensitizer Zn phthalocyanine (ZnPc) loaded in ultradeformable liposomes (UDL-ZnPc) both in the darkness and upon sunlight irradiation and screened the ability of UDL-ZnPc to penetrate intact skin.

2. Materials and methods

2.1. Materials

Soybean phosphatidylcholine (SPC) (phospholipon 90 G, purity >90%) was a gift from Phospholipid/Natterman, Germany. Sodium cholate (NaChol), 1,2-Dimyristoyl-*sn*-glycero-3-phosphoethanolamine-N-(Lissamine™ rhodamine B sulfonyl) (Rh-PE), and Sephadex G-50 were purchased from Sigma-Aldrich, Argentina. The fluorophore 8-hydroxypyrene-1,3,6-trisulfonic acid (HPTS) was from Molecular Probes (Eugene, OR, USA). Q-tracker non-targeted Quantum Dots 655, with a *core/shell* of CdSe/ZnS covered by PEG (QD) was from Invitrogen (Hayward, CA). The hydrophobic ([tetrakis(2,4-dimetil-3-pentyloxi)-phthalocyaninate]zinc(II)) Zn phthalocyanine (ZnPc) was synthesized as described in Montanari et al. [27]. Other reagents were analytic grade from Anedra, Argentina.

2.2. Preparation and characterization of ultradeformable liposomes

UDL and UDL-ZnPc were prepared as stated in Montanari et al. [27]. Briefly, UDL composed of SPC and NaChol at 6:1 (w/w) ratio, were prepared by mixing lipids from $CHCl_3$ and $CHCl_3$:CH_3OH (1:1, v/v) solutions, respectively, that were further rotary evaporated at 40 °C in round bottom flask until organic solvent elimination. The thin lipid film was flushed with N_2, and hydrated in 10 mM Tris–HCl buffer plus 0.9% (w/v) NaCl, pH 7.4 (Tris buffer), up to a final concentration of 43 mg SPC/ml. The suspension was sonicated (45 min with a bath type sonicator 80 W, 40 kHz) and extruded 15 times through two stacked 0.2 and 0.1 μm pore size polycarbonate filters using a 100 ml Thermobarrel extruder (Northern Lipids, Canada). ZnPc was co-solubilized in the organic solution with lipids (2 mg ZnPc/g SPC) to prepare UDL-ZnPc.

Conventional – non ultradeformable, without NaChol – liposomes (L) were prepared by the same procedure.

Liposomal phospholipids were quantified by a colorimetric phosphate micro assay [28]. Mean particle size and Z potential of each liposomal preparation were determined by dynamic light scattering with a Nanozetasizer (Malvern).

2.3. Cytotoxicity on mammal cells

2.3.1. Lactate dehydrogenase (LDH) assay

J774 and Vero cells were maintained at 37 °C with 5% CO_2, in RPMI 1640 medium supplemented with 10% heat-inactivated FCS, 2 mM glutamine, 100 UI/ml penicillin and 100 μg/ml streptomycin (PE/ST) and amphotericin (all from Invitrogen Corporation). Culture medium of nearly confluent cell layers was replaced by 100 μl of medium containing UDL (1 and 10 mM phospholipids). Upon 1 h incubation at 37 °C, suspensions were removed; cells were washed with PBS (140 mM NaCl, 8.7 mM Na_2HPO_4, 1.8 mM NaH_2PO_4, pH 7.4) replaced by fresh RPMI medium and cells were incubated for 24 h at 37 °C. Upon incubation, supernatants were transferred to fresh tubes; centrifuged at 250 ×*g* for 4 min and LDH content was measured using lactate dehydrogenase CytoTox Kit (Promega) [29]. LDH concentration was expressed as percentage LDH release relative to treatment with the detergent Triton X-100 and then percentage of viability was calculated considering the LDH leakage of cells grown in medium.

2.3.2. Glutathione assay (GSH)

Total cellular glutathione of J774 cells was measured using the Tietze method [30]. Culture medium of nearly confluent J774 cells was replaced by 100 μl of medium containing free ZnPc (1.25 and 12.5 μM), UDL (1 and 10 mM) or UDL-ZnPc (1.25 μM ZnPc–1 mM phospholipids and 12.5 μM ZnPc–10 mM phospholipids). Upon 24 h incubation at 37 °C, suspensions were removed, replaced by fresh RPMI medium and one plate was exposed to direct sunlight along 15 min (light dose of 15 J/cm^2 at λ = 600–650 nm measured by Radiometer Laser Mate Q, Coherent), meanwhile other plate was kept in the dark. After treatments, cell were incubated for 24 h at 37 °C, then media were removed and cells were washed with PBS and collected into eppendorf tubes by trypsin treatment. Then trypsin was inactivated, cells were twice washed with PBS by centrifugation and finally suspended in 100 μl of 1 mM EDTA. Cells were lysed by sonication (tip sonicator 10 s) and cellular debris were removed by centrifugation (10000 ×*g* for 15 min at 4 °C). 20 μl aliquots of each supernatant were transferred to 96 wells plates for glutathione determination. The reaction was started by adding 180 μl of reaction mixture [60 μM 5,5′-dithio-*bis*(2-nitrobenzoic acid) (DTNB), 1.5 mM NADPH, 0.1 mM EDTA, and 2.4 U/ml GSH reductase in $NaHCO_3$ 0.1% (all from Sigma-Aldrich, St. Louis, MO, USA)]. Absorbance at 412 nm was monitored after 15 min with a microplate reader and the glutathione concentration was determined by comparing the rate of colour change with that of a GSH standard curve.

2.4. UDL-ZnPc internalization by promastigotes

Leishmania braziliensis promastigotes (STRAIN 2903) were cultured at 25 °C in Novy–McNeal–Nicolle biphasic medium [31] and RPMI 1640 supplemented with 10% FCS and PE/ST. Before treatments, promastigotes were taken from liquid phase and transferred to RPMI medium.

L. braziliensis promastigotes were incubated with UDL-ZnPc (1.25 μM ZnPc-1 mM phospholipids) for 15 min at 4 °C and 25 °C. Upon incubation, parasites were washed by centrifugation (3830 ×*g* for 3 min) and fixed in 2% v/v formaldehyde in PBS. The emission of ZnPc was monitored with a confocal laser scanning microscope (CLSM) Olympus FV300 equipped with a He–Ne 633 nm laser.

2.5. Anti-promastigote activity

Promastigotes were incubated for 5 min at 25 °C with empty L and UDL (1 and 0.1 mM phospholipids) (100 μl RPMI with 10% FCS and PE/ST). Upon incubation, samples were centrifuged (3800 ×*g* for 10 min at 20 °C), supernatants were removed and replaced by fresh RPMI medium. Parasites were further incubated for 3 h at 25 °C and mobility was evaluated microscopically.

Promastigotes (5×10^5) were incubated for 30 min at 25 °C with empty UDL (1 mM phospholipids), free ZnPc (1.25 μM), UDL-ZnPc and L-ZnPc (both 1.25 μM ZnPc-1 mM phospholipids). Upon incubation, samples were centrifuged (3800 ×*g* for 10 min at 20 °C),

supernatants were removed and replaced by fresh RPMI medium, and exposed 15 min to direct sunlight as stated before. Control cells were maintained on the dark. After treatments, parasites were incubated for 24 h or 48 h at 25 °C and inhibition of promastigotes growth was microscopically determined by counting parasite numbers in a Neubauer haemocytometer. Anti-promastigote activity was expressed as: % APA = [1 − (no. of promastigotes treated) / (no. of promastigotes control)] × 100.

2.6. Intracellular anti-amastigote activity

RAW macrophages maintained in RPMI 1640 medium supplemented with 10% FCS and PE/ST grown to nearly confluence on rounded coverslips in 24-well plates were infected with *Leishmania* promastigotes at 1:10 macrophage: promastigotes ratio, and the following treatments were done: a. 24 h incubation with UDL-ZnPc (1.25 μM ZnPc–1 mM phospholipids) or ZnPc (1.25 μM); b. 2 h incubation with UDL-ZnPc, ZnPc or empty UDL followed by 22 h incubation in RPMI medium; c. 22 h incubation only with promastigotes followed by 2 h incubation with UDL-ZnPc or ZnPc. After incubation in the dark, suspensions were removed, replaced by fresh RPMI medium and exposed to direct sunlight along 15 min as described above. Control cells were maintained on the dark. After 24 h, the coverslips were removed, washed with PBS, fixed with methanol and stained with Giemsa. The number of amastigotes/300 cells was counted by using light microscopy. Untreated infected macrophages were used as control. Anti-amastigote activity was expressed as: % AA = [1 − (no. of amastigotes/100 cells) treated / (no. of amastigotes/100 cells) control] × 100.

2.7. In vitro skin penetration studies

Excised human skin from Caucasian female patients, who had undergone abdominal plastic surgery, was used. Patients were healthy and with no medical history of dermatological disease. After excision, the skin was cut into $10 \times 10\ cm^2$ pieces and the subcutaneous fatty tissue was removed from the skin specimen using a scalpel. Afterwards the surface of each specimen was cleaned with water, wrapped in aluminum foil and stored in polyethylene bags at −26 °C until use. Previous investigations have shown that no change in the penetration characteristics occurs during the storage time of 6 months [32,33].

Disks of 24 mm in diameter were punched out from frozen skin, thawed, cleaned with PBS solution, and transferred directly into the Saarbrücken Penetration Model (SPM). Briefly, the skin was put onto a filter paper soaked with Ringer solution and placed into the cavity of a Teflon block.

UDL and L containing HPTS (UDL-HPTS and L-HPTS) were prepared as stated in Section 2.2, excepting that the lipid films were hydrated with a solution containing 35 mM HPTS in Tris–HCl buffer. After extrusion the free HPTS was eliminated by gel permeation chromatography in a Shepadex G-50 column using the minicolumn centrifugation method [34].

UDL-HPTS or L-HPTS (11 μl/cm^2 corresponding to 0.12 mg phospholipids/cm^2 and same amount of HPTS) were applied to the skin surface, the system was placed into an oven at 35 °C, and were incubated for 1 and 5 h after drying of the vesicle solutions. Besides, UDL-ZnPc, L-ZnPc and free ZnPc solubilized in DMSO were applied to the skin disks at 2.58 nmol of ZnPc/cm^2, placed at 35 °C and incubated for 1 h after drying of the suspensions.

2.7.1. Skin segmentation

After incubation time the skin specimens mounted on SPM were segmented using tape stripping method or optically scanned by CLSM.

2.7.1.1. Tape stripping. After the incubation time skin specimens were segmented using tape stripping method as described by Wagner [35]. Briefly, the formulation was wiped off from the skin surface using cotton. Then the skin piece was mounted on an extruded polystyrene foam disc using small pins to stretch the tissue and covered with a teflon mask with a central hole of 15 mm in diameter for the HPTS formulations and successively stripped with 20 pieces of adhesive tape (Scotch 3 M) placed on the central hole, while for the ZnPc formulations the tapes were placed covering the whole surface of the skin segments. Each tape was charged with a weight of 2 kg per 10 s and rapidly removed.

HPTS was extracted from each tape with 3 ml of ethanol–water (1:1 v:v), shaken at 190 rpm for 1 h at 37 °C. Emission of HPTS (510 nm) was measured upon excitation at 453 nm, using a Perkin-Elmer LS 55 spectrofluorometer.

ZnPc from the twenty tapes was extracted overnight with 4 ml of DMSO at room temperature. Emission of ZnPc at 710 nm was measured upon excitation at 699 nm [36]. Calibration curves were prepared among each experiment to quantify ZnPc, showing linear behavior between 0.01 and 0.2 μmol/l with a correlation coefficient (r^2) of 0.999.

After the tape stripping, the remaining skin below the stratum corneum (SC) – i.e. the viable epidermis and the dermis – was cut into small pieces, placed into 4 ml of DMSO, homogenized, sonicated for 20 min, filtered and the fluorescence was measured the same as for the tapes [36].

2.7.1.2. Optical scanning. After incubation, the full skin thickness was optically scanned at 2 μm increments through the z-axis by CLSM equipped with an Ar laser (488 nm). Fluorescence intensity of each image was obtained by Image-J software.

2.7.2. Skin cryosectioning

UDL and L containing HPTS and Rh-PE or ZnPc (UDL-HPTS-Rh-PE/ZnPc and L-HPTS-Rh-PE/ZnPc) were prepared as stated in Section 2.2, excepting that Rh-PE (1: 1000, Rh-PE: SPC, mol:mol) or ZnPc were co-solubilized in organic solution with lipids. UDL containing Quantum Dots (UDL-QD) were prepared by hydrating the thin lipid film with a suspension of 0.01 nmol QD/ml in Tris-HCl buffer. Negative staining electron microscopy images of liposomes upon uranyl acetate staining were obtained with a JEOL JEM 1200 EX II microscope.

Formulations were applied to the skin surface and incubated for 1 h in a SPM as stated before (Section 2.7). After incubation the skin was rapidly frozen in dry ice, embedded in OCT and sliced in sections of 8 μm thickness, perpendicular to the skin, with a cryomicrotome Reichert-Jung CryoCut 1800 (Germany). Skin slices were fixed with 10% formaldehyde and observed by CLSM equipped with an Ar laser (488 nm for HPTS and QD excitation) and a He–Ne laser (543 nm for Rh-PE and ZnPc excitation).

The same specimens were also subjected to hematoxylin and eosin staining in order to detect the possible presence of histological alterations in the analyzed tissues, using light microscopy.

2.8. Statistical analysis

The significance of the differences between the mean values of studied parameters was determined using the Student's *t*-test.

3. Results

3.1. Liposomal characterization

The preparations rendered ULD-ZnPc (58 nmol ZnPc/52 μmol phospholipid/ml) of 99.9 ± 1.2 nm in size with unimodal distribution and a Zeta potential of −36.7 ± 3.8. Similar results were obtained for L-ZnPc (44 nmol ZnPc/44 μmol phospholipid/ml).

3.2. Cytotoxicity on mammal cells

The effect of empty UDL on cell membrane integrity of fibroblasts (Vero cells) and of macrophages (J774 cells) was determined by LDH leakage. UDL at 1 mM phospholipids did not induce LDH leakage on both cell types, although at 10 mM caused 80% leakage of LDH on J774 cells upon 1 h incubation (Fig. 1a). L did not produce LDH leakage either at 1 or 10 mM (data not shown). Additionally, total GSH level in J774 cells was measured upon incubation with UDL-ZnPc followed by sun irradiation. GSH level was not altered after incubation with free ZnPc, (12.5 μM) empty UDL (10 mM) or UDL-ZnPc (1 mM phospholipids–1.25 μM ZnPc) in the dark or after irradiation. Although, GSH was significantly diminished upon incubation of UDL-ZnPc at 10 mM phospholipids–12.5 μM ZnPc followed by 15 min of sun irradiation (Fig. 1b).

3.3. UDL-ZnPc internalization by promastigotes

L. braziliensis promastigotes were incubated with UDL-ZnPc at 25 °C (optimum temperature of growth) and at 4 °C (temperature at which internalization by endocytic uptake is absent due to reduced metabolism of cells [37]) to distinguish between active uptake and superficial adsorption. Fluorescence microscopy showed higher intensity of fluorescence upon incubation at 25 °C than at 4 °C (Fig. 2). These results could suggest that UDL-ZnPc were internalized by promastigotes by endocytic uptake.

3.4. Anti-promastigote activity

First, it was observed that around 17 and 29% of promastigotes lost motility upon incubation with L at 0.1 and 1 mM, respectively, while the rest of the parasites kept highly mobile. Although, 5 min incubation with UDL induced an important diminish of motility. 90% of parasites lost motility after incubation with UDL at 0.1 and 1 mM, meanwhile the rest of the parasites kept highly mobile (0.1 mM) or with low motility (1 mM).

Then, to determine if lost of motility was related with loss of viability, anti-promastigote activity (APA) was determined after 30 min incubation followed by 24 or 48 h of parasite growth. First, empty UDL and UDL-ZnPc in the dark showed high and similar APA of around 80% after 24 h of growth. Nevertheless, the highest anti-promastigote effect (100% APA) was shown upon 15 min of sun irradiation of promastigotes treated with UDL-ZnPc (Fig. 3). Upon 48 h of parasite growth, all the treatments showed APA of around 100%.

On the other hand, free ZnPc at 1.25 μM did not affect the motility of promastigotes upon 5 min incubation and it showed 20% APA after sun irradiation and 48 h of parasite growth, while L-ZnPc showed 0% APA in the darkness or upon irradiation (data not shown).

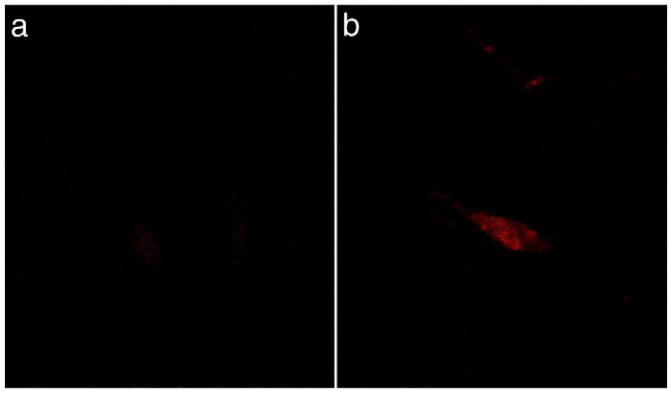

Fig. 2. CLSM images of *L. braziliensis* promastigotes incubated with UDL-ZnPc at 4 °C (a) and 25 °C (b).

3.5. Intracellular anti-amastigote activity

Anti-amastigote activity (AA) was determined in two ways: first, samples were co-incubated for 2 or 24 h with RAW macrophages and promastigotes and second, samples were incubated for 2 h with macrophages previously infected.

Empty UDL had insignificant AA (5%), meanwhile activity of free ZnPc and UDL-ZnPc increased as time of incubation increased from 2 to 24 h (Fig. 4a). While free ZnPc showed activity only upon irradiation (20 and 35% AA after 2 and 24 h, respectively), when incorporated in UDL (UDL-ZnPc) activities in the dark or upon irradiation were not different (AA 40 and 80% after 2 and 24 h, respectively), but were almost the double of AA for free ZnPc.

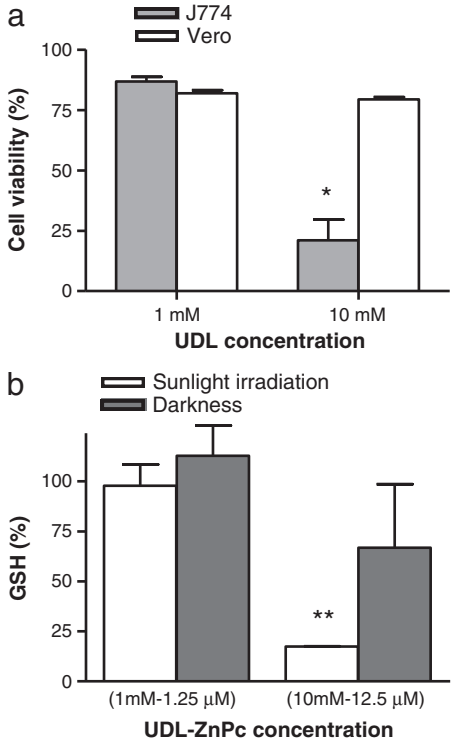

Fig. 1. Mammal cells cytotoxicity measured as LDH leakage induced by UDL on J774 and Vero cells upon 1 h incubation (a) and GSH content in J774 cells after incubation with UDL-ZnPc in the dark or upon irradiation (b). Each data point represents the mean ± standard deviation ($n=3$). *$p<0.05$, **$p<0.01$.

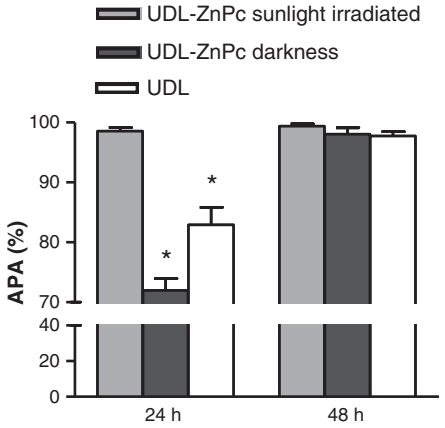

Fig. 3. Anti-promastigote activity (APA%) of UDL and UDL-ZnPc in the dark or upon 15 min sunlight irradiation. *$p<0.05$.

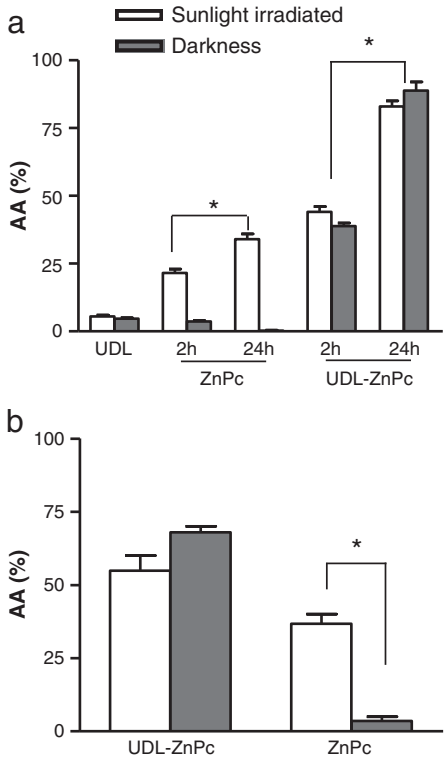

Fig. 4. Anti-amastigote activity (AA%) of UDL, ZnPc and UDL-ZnPc co-incubated with RAW macrophages and *L. braziliensis* promastigotes for 2 or 24 h (a), and of UDL-ZnPc and ZnPc incubated with RAW macrophages previously infected with *L. braziliensis* promastigotes for 2 h (b). Cells were then exposed to 15 min sunlight irradiation or maintained in the dark and grown for 24 h. *$p<0.05$.

Finally, free ZnPc as well as UDL-ZnPc showed AA upon 2 h incubation with infected macrophages (Fig. 4b). Again, free ZnPc activity was irradiation dependent (3 vs 36% AA, in the dark and after irradiation, respectively), while UDL-ZnPc activity was independent (55% AA) and higher than AA of free ZnPc.

3.6. In vitro skin penetration studies

Skin penetration of the hydrosoluble fluorescent dye HPTS encapsulated in UDL and L was determined using the SPM followed by segmentation by tape stripping or optical scanning by CLSM up to 60 μm depth. The presence of ZnPc in SC and in deeper viable epidermis and dermis upon incubation as free ZnPc, UDL-ZnPc and L-ZnPc was also quantified. Finally, skin penetration of HPTS and the hydrophobic Rh-PE or ZnPc co-encapsulated in UDL and L were recorded by cryosectioning to assess the integrity of vesicles along penetration.

SPM was employed under non-occlusive conditions, in order to maintain the humidity gradient across the skin, that it is proposed to be the locomotive force for UDL penetration [38]. If compared with Franz diffusion cell, SPM avoids the non-physiological hydration and changes of the skin due to the absence of liquid as receptor medium. This system, coupled to segmentation techniques, such as tape stripping or cryosectioning, allows the measurement of penetration profiles of drugs with respect to the depth of the tissue. To avoid the reported variability of the tape stripping [39–41], the experiments were carried out with the same skin donor, repeated 5 times and the distance and geometry of skin fixation – responsible for maintaining the stretching of the skin during tape stripping – were kept constant.

Fluorescence profiles of UDL-HPTS and L-HPTS extracted from each strip upon 1 h incubation were significantly different (Fig. 5). The cumulative of fluorescence in the 20 strips (corresponding to the total SC), was around 6.8 folds higher for UDL-HPTS than for L-HPTS

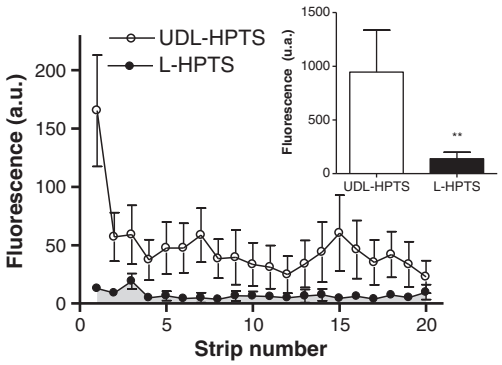

Fig. 5. SC strip profile of HPTS after 1 h of non-occlusive application of UDL-HPTS or L-HPTS ($n=5$). Inset: Cumulative fluorescence in the 20 strips. **$p<0.01$.

(Inset Fig. 5). Fluorescence profiles and accumulated fluorescence upon 5 h incubation were similar to those obtained after 1 h of incubation, for both formulations.

In this procedure, each removed cell layer had nearly the same thickness [35,42] being the number of tape strips linearly correlated with the remaining thickness of the SC. According to this, UDL-HPTS penetrated deeper into the SC than L-HPTS.

The optical scanning (Fig. 6) showed that HPTS distributed in SC layers in patterns similar, but slightly thicker than the net of nanochannels previously described [43,44].

The use of SPM ensured that the detected fluorescence was exclusively owed to the penetration of HPTS, Rh-PE or ZnPc from top to bottom at the lower layers of the epidermis, and not to the basolateral penetration which is inherent to the Franz cell [35].

Transversal skin cryosections after 1 h incubation with double fluorescently labeled liposomes (UDL-HPTS-Rh-PE/ZnPc or L-HPTS-Rh-PE/ZnPc), showed maximal fluorescence intensity of Rh-PE/ZnPc from UDL at the first 8 μm up to a depth of 14 μm, in the boundaries of the viable epidermis (8–13 μm [45]). Based on the osmotic force theory of Cevc and Blume [46], the UDL would not penetrate beyond the non-hydrated deepest layers of the SC. The hydrophilic HPTS

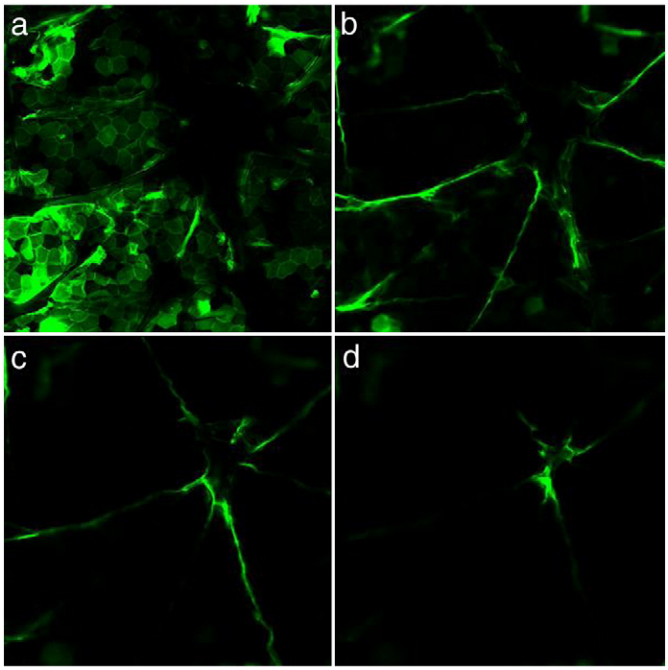

Fig. 6. Typical series of CLSM images obtained horizontally at 0 μm (a), 20 μm (b), 40 μm (c) and 60 μm (d) from skin surface upon1 h incubation with UDL-HPTS.

however, was found in a separate fraction, entering the viable epidermis, up to a mean depth of 24 μm (Fig. 7a and b). On the contrary, fluorescence of Rh-PE/ZnPc from L was only detected at the first 1 μm (first SC cells layer), while a slight diffuse poorly intense fluorescence from HPTS was found up to 2 μm (Fig. 7c and d).

After 1 h incubation in SPM of 11.7 nmol ZnPc (dissolved in DMSO at 0.98 μmol/ml)/4.5 cm^2 total area, followed by removal of material remaining on the skin surface, it was found that only 1 out of 5 skin specimens contained ZnPc in quantitative amounts within SC, viable epidermis and dermis (data not shown). On the contrary, upon applying the same amount of ZnPc/4.5 cm^2 either as UDL-ZnPc or L-ZnPc, it was found that UDL-ZnPc delivered 7.35 folds higher amount of ZnPc than L-ZnPc. As judged by the penetration profile of Rh-PE/ZnPc in Fig. 7 it was reasonably to assume that the UDL-ZnPc (lipid matrix and ZnPc) homogeneously distributed across the ~8 μm thickness of the SC, whereas L-ZnPc remained stacked on the first layer of the SC. In other words, upon applying the same amount of ZnPc/surface, $\sim 3.8\times10^{-2}$ nmol UDL-ZnPc were evenly distributed in a volume of [1 cm^2 surface $\times 8\times10^{-4}$ cm depth] of SC, while $\sim 5.4\times10^{-3}$ nmol L-ZnPc distributed in a volume of [1 cm^2 surface $\times 1\times10^{-4}$ cm depth]. Hence, UDL-ZnPc rendered nearly 7 folds more quantity of ZnPc within the SC, distributed in a cylinder 8 folds more profound than L-ZnPc. Assuming an homogeneous distribution, the concentration of UDL-ZnPc within the whole depth of SC was 47 μM, far beyond the concentration that *in vitro* was necessary to kill promastigotes upon 15 min sunlight irradiation. UDL-ZnPc also rendered nearly 40 folds higher amount ZnPc (8.63×10^{-3} nmol) distributed across the remainder viable epidermis and dermis, than L-ZnPc (Fig. 8). Again, only 1 out of 5 skin specimens showed a significant presence of ZnPc within the rest of skin when it was applied in DMSO solution (data not shown).

Finally, the penetration profile of QD and UDL-QD was determined. The UDL-QD suspension was translucent with a mean vesicular size of 102 nm and polydispersity index of 0.128 (Fig. 9a and b). After 1 h incubation, the fluorescence of QD was distributed both across the SC as well across the viable epidermis (Fig. 10a) in coincidence with other authors [47], whereas that of UDL-QD remained confined in the thickness of the SC (Fig. 10b).

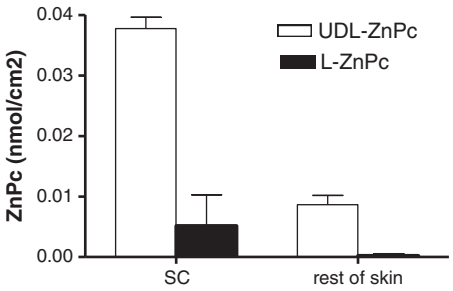

Fig. 8. Penetration of ZnPc in skin layers after 1 h non-occlusive incubation with UDL-ZnPc and L-ZnPc.

4. Discussion

In vitro, aminolevulinic acid (ALA)-PDT fails in eliminate the intracellular Leishmania amastigotes. For instance, 4 h incubation with ALA followed by irradiation with a 635 nm laser up to 50 J/cm^2 of *L. major* infected J774 cells, reduces the number of J774 cells but does not diminish the number of intracellular parasites [48]. The reason for this is that only mammal host cells can metabolize the ALA precursor to the photosensitizer protoporphyrin IX (PpIX). PpIX is further accumulated inside the intracellular amastigotes in an amount insufficient to kill the parasites at fluence of 10 J/cm^2. The phototoxic effect against parasites occurs at a high concentration of PpIX ($LD_{50}\approx 3.8\times10^{-4}$ M), that cannot be applied *in vivo* without generating serious toxic side effects. Clinically however, succeeded application of ALA- and MAL-PDT to CL patients caused by *L. donovani* and *L. major*, have been published in 2003 and 2004 [49–51]. Recently, it was shown that lesions healed rapidly with good cosmetic results in a patient with facial cutaneous *L. tropica* infection resistant to various therapeutic regimes after MAL-PDT treatment [23] and improved results were found in a comparative study between ALA-PDT and topical paromomycin [52]. It is feasible that *in vivo* the induction of a local immune response (for instance increased levels of IL-6) leading to a non-specific tissue damage accompanied by macrophages elimination, should account for the success of the ALA-PDT [48]. In other words, the leishmanicidal effect is mediated by an immune host reaction against a non-specific photochemical damage, and not by a selective effect exclusively elicited by the PDT.

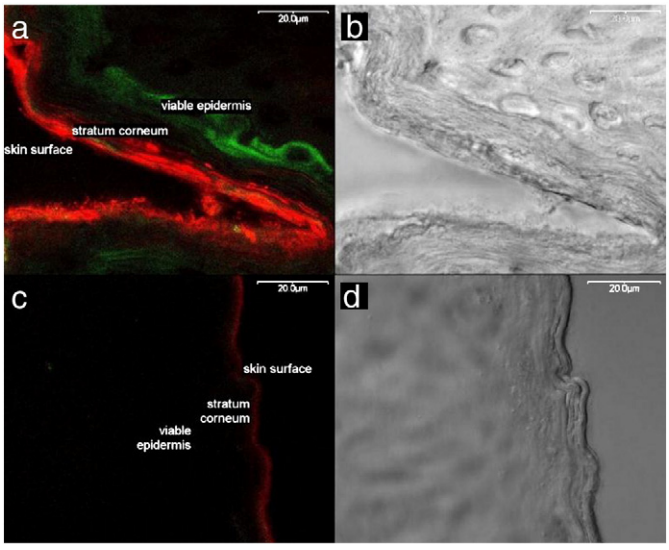

Fig. 7. CLSM images of cryosectioned skin after 1 h incubation with UDL-HPTS-rh-PE (a and b, fluorescence and the corresponding differential interference contrast image, respectively) and with L-HPTS-rh-PE (c and d, fluorescence and the corresponding differential interference contrast image, respectively). Red and green signals from rh-PE and HPTS, respectively.

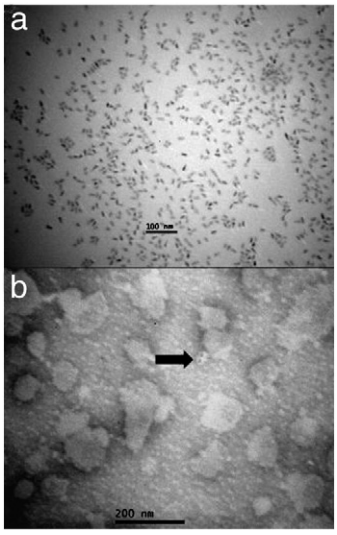

Fig. 9. Transmission electron microscopy images of free QD (a) (ellipsoidal shape, 6 nm short axe, 12 nm long axe and hydrodynamic diameter due to polyethylene glycol coverage up to 45 nm [68]) and UDL-QD (b). Arrow points to QD contained inside UDL.

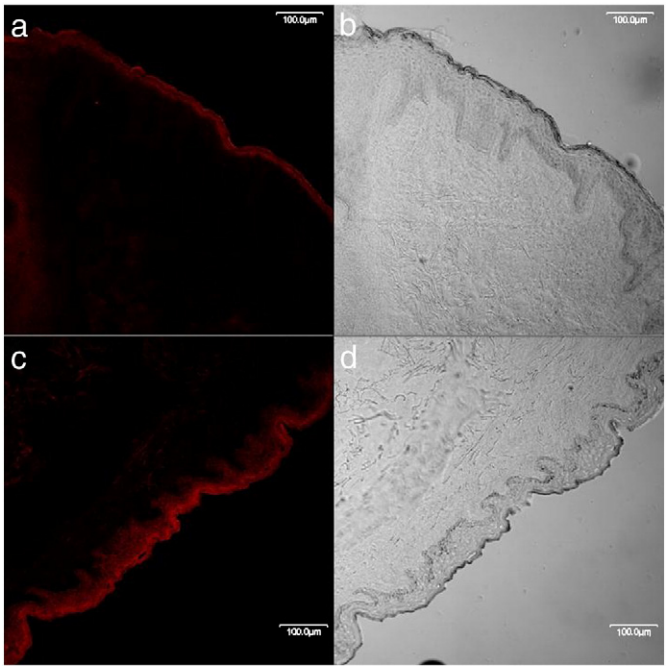

Fig. 10. CLSM images of cryosectioned skin after 1 h of incubation with UDL-QD (a and b, fluorescence and the corresponding differential interference contrast image, respectively) and with QD (c and d, fluorescence and the corresponding differential interference contrast image, respectively).

Different photosensitizers such as phenothiazinium, aluminum chloride phthalocyanine and zinc phthalocyanine (with direct action in their intact form), also have shown succeeding preclinical results in the last four years [53,54]. In particular, results from Dutta indicates that promastigotes and axenic amastigotes of *L. amazonensis* are more sensitive than J774 macrophages to light-mediated cytolysis at low concentration (1 μM) of the hydrophobic aluminum phthalocyanine chloride (AlPhCl) under a low energy dose (1.5 J/cm^2). Nevertheless, AlPhCl had no AA on infected J774 cells, and intracellular amastigotes could be eliminated only when AlPhCl was previously incubated with axenic amastigotes before the macrophages were infected [55]. This fact suggested that the cell membrane could hinder the free access of AlPhCl to intracellular targets.

A suitable delivery system could help to overcome the tissue and cellular barriers interposed between hydrophobic phthalocyanines and target amastigotes. Actually, the co-localization of phthalocyanine and target in a small volume of space should be the key to optimize the photodynamic activity, because of the short half life (<0.1 ms) and small action radii (10–20 nm) of singlet oxygen [56]. However, changing both the internalization mechanism and the intracellular traffic of the phthalocyanine (free phthalocyanine diffuse across the plasma membrane, and then relocate to other intracellular membranes [57]) by means of a delivery system could also arise unexpected toxic effects.

With the aim of improving the penetration of the hydrophobic ZnPc across the intact SC without using organic solvents and to count on a particulate vehicle with increased chances of being selectively captured by infected macrophages in the skin, we had previously characterized and determined the photochemical parameters of ZnPc loaded in a highly hydrophilic ultradeformable lipid matrix. When partitioned in UDL bilayers, ZnPc remains in monomeric form and exhibit similar photodynamic properties than in organic solvents, as judged by the similar value of the singlet oxygen quantum yield from UDL-ZnPc and ZnPc in ethanol. Upon UDL-ZnPc internalization, the phago/lysosomal compartment of macrophages remains intact after 15 min of sunlight irradiation. Cytotoxicity, as measured by the MTT assay on Vero and J774 cells, is absent up to 10 μM free ZnPc, as well as for up to 18 mM empty UDL, both in the dark or after 15 min sunlight irradiation. UDL-ZnPc at 10 μM ZnPc–8 mM phospholipids however, reduces 75% J774 cell viability, not only after irradiation but also in the dark [27].

In this work the GSH levels and release of cytosolic LDH were tested to delimit a safe threshold concentration of UDL and UDL-ZnPc when incubated with host phagocytes. The crucial factors determining the type of cell death following PDT are cell type, the subcellular localization of the photosensitizer, and the light dose applied [58] (lower doses – such as the one received upon 15 min sunlight irradiation – lead to more apoptotic cells, while higher doses result in more necrotic cells [59]). Diminished GSH (the principal intracellular low-molecular-weight thiol that plays a critical role in the cellular defence against oxidative and nitrosative stress in mammalian cells) levels are observed in the early stages of apoptosis [60]. We found that 1.25 μM free ZnPc or as UDL-ZnPc and 1 mM phospholipids empty UDL did not diminish the intracellular GSH level in J774 cells, neither in the darkness nor after 15 min sunlight irradiation. The presence of 30 mol% of the detergent sodium cholate within the UDL matrix could induce membrane damages when in contact to host cell surface, but 1 mM phospholipids empty UDL did not induce the release of LDH neither by Vero nor J774 cells. At 10 mM of phospholipids however, an important release of LDH was produced by J774 cells, which was absent at the same concentration of L. The faster uptake rate of phagocytosis, leading to higher amounts of internalized detergent in comparison to endocytosis [61], could be the reason for this non-photodynamic damage caused by UDL on J774.

The leishmanicidal activity was tested at 1 mM phospholipids and 1.25 μM ZnPc upon 15 min sunlight irradiation since neither photodynamic nor non-photodynamic damage as measured by MTT, LDH assays and GSH consumption by phagocytic cells was registered below these threshold concentrations. Only 5 min incubation at 25 °C was sufficient for empty UDL to produce an important decrease in motility of promastigotes. Same sized L neither caused relevant effect on parasite motility nor was captured by promastigotes, in accordance with previous results indicating that submicron diameter L can only be absorbed on the surface of cell parasites [62]. The intense fluorescence signal from UDL-ZnPc associated to the parasite upon 15 min incubation at 25 °C suggested an active uptake of UDL. The cytoskeleton of *Leishmania* promastigote is organized as a microtubule network underlying the cell membrane. The only available area for exchange of macromolecules with the external environment is the nearly 1 μm^2 surface of the flagellar pocket [63,64]. The elastic modulus of UDL is twenty folds lower than that of L, allowing for micro/nanoscaled spontaneous fluctuations of the bilayer at room temperature [65]. This could facilitate its endocytic uptake by the flagellar pocket. Hence the lipid matrix ultradeformability leading to its internalization and parasite immobilization could be the source of the observed non-photodynamic leishmanicidal activity.

On the other hand, UDL-ZnPc showed 100% APA (five folds increased over that of free ZnPc) after 15 min sunlight irradiation. Both UDL-ZnPc in the darkness as well as empty UDL also exhibited around 80% APA, while ZnPc and L-ZnPc did not (this last even after sunlight irradiation). These facts indicated that a high APA could simply be induced by internalization of empty ultradeformable matrices. For UDL-ZnPc, the irradiation yet contributed to accelerate the leishmanicidal effect upon internalization.

As UDL-ZnPc, AA raised up to 80% (more than two folds increased over that of the strictly sunlight dependent AA of free ZnPc) when co-incubated with promastigotes and RAW macrophages along 24. Remarkably, AA of UDL-ZnPc was independent of irradiation. Part of the 80% AA could arise from APA caused by UDL/UDL-ZnPc before infecting the RAW cells. In other words, probably the observed AA aroused from an infection occurred with a lower amount of viable parasites that the stated in the experimental method.

Taken together, though formerly aimed for PDT, these results indicated that an important part of the UDL-ZnPc leishmanicidal activity was independent of the irradiation. As previously discussed, the empty ultradeformable lipid matrix was an effective non-photodynamic leishmanicidal agent that fully manifested as *in vitro* APA. The *in vitro* AA of UDL was absent, but the non-photodynamic AA from UDL-ZnPc was unexpectedly high. And explanation for this could be that phagocytosis of UDL-ZnPc by host cells resulted in products that were innocuous for the host but lethal for the parasites.

As previously observed by Cevc [38] and Honeywell–Nguyen [44], we determined that the hydrophobic Rh-PE or ZnPc and the hydrophilic HPTS when loaded in UDL rapidly entered the SC, but did not if loaded in L. Also in accordance to Honeywell–Nguyen [40,66] who determined that a hydrophilic drug is released from the lipid matrix diffusing to deeper layers in the epidermis, the hydrophobic molecules Rh-PE/ZnPc were found at the SC-viable epidermal junction, while HPTS was found deeper in the epidermis. At the end of the SC, the hydrophilic molecules were shuttled from the carrier.

Our results indicated that UDL-ZnPc penetrated homogeneously in the SC, carrying 7 folds higher amount of ZnPc 8 folds deeper than L-ZnPc while ZnPc in DMSO did it in a poorly reproducible fashion after 1 h incubation. Three weeks is the elapsed time for desquamation and renewal of SC [67] and probably within that period the UDL-ZnPc concentrated in SC would act as a reservoir for delivery of lipid matrix and ZnPc to the viable epidermis. Remarkably, the UDL-ZnPc was the only formulation ensuring a reproducible and quantitative delivery of ZnPc to the viable epidermis and dermis upon a single application and 1 h incubation. This amount could be increased after multiple applications. Infected macrophages can be found at different levels within the viable epidermis and clearly UDL-ZnPc showed to be a suitable tool to increase the amount of ZnPc delivered into and beyond the SC, as judged by this *in vitro* assay.

Infected macrophages are specialized in the uptake of particulate material. Hence the chances of being internalized should be increased as long as the vesicular integrity of UDL-ZnPc is conserved. Since the high sized ellipsoidal QD remained trapped into the relatively small (100 nm diameter) UDL matrix, probably the vesicular structure of the UDL were conserved along the SC penetration. Otherwise the QD should squeeze deeper into the epidermis, as the free QD did. Hence, excluding the use of organic solvents such as dimethylsulphoxide or dimethylformamide that are required to dissolve highly hydrophobic molecules like ZnPc, we could reasonably expect that in spite of the loss of hydrophilic content across the SC penetration, the ZnPc-UDL could get close to the viable epidermis in an – at least – partly particulate form.

Further studies will reveal if these UDL when applied in minimal doses on the surface of intact skin could have a preventive or therapeutic effect aroused both from their photodynamic activity as well as from their non-photodynamic activity during the first stages of the infection. It is likely that the leishmanicidal effect upon transcutaneous application of UDL could result from a synergistic effect fruit from its multiple leishmanicidal activity and its superior capacity of penetration.

Acknowledgements

This work was supported by a grant from the Secretaria de Investigaciones, Universidad Nacional de Quilmes, and from the Comisión de Investigaciones Científicas de la Provincia de Buenos Aires. MJ Morilla and EL Romero are members of the Carrera del Investigador Científico del Consejo Nacional de Investigaciones Científicas y Técnicas, Argentina (CONICET). J Montanari has got a fellowship from CONICET. Dr H Jimenez provided the skin explants from surgery. Students LA Lado and L Rivadeneyra collaborated in the development of the skin experiments.

References

[1] R. Bonfante, S. Barruela, Leishmanias y Leishmaniasis en América con especial referencia a Venezuela, Tipografía y Litografía Horizonte C.A., Caracas, 2002.
[2] S. Jeronimo, A. de Queiroz Sousa, R. Pearson, in: R. Guerrant, D. Walker, P. Weller (Eds.), Tropical Infectious Diseases: Principles, Pathogens and Practice, Churchill Livingstone Elsevier, Edinburgh, Scotland, 2006, pp. 1095–1113.
[3] B.L. Herwaldt, Leishmaniasis, Lancet 354 (9185) (1999) 1191–1199.
[4] WHO, Leishmaniasis, , 2004.
[5] C.R. Davies, E.A. Llanos-Cuentas, S.J. Sharp, J. Canales, E. Leon, E. Alvarez, N. Roncal, C. Dye, Cutaneous leishmaniasis in the Peruvian Andes: factors associated with variability in clinical symptoms, response to treatment, and parasite isolation rate, Clin. Infect. Dis. 25 (2) (1997) 302–310.
[6] C. Bern, J.H. Maguire, J. Alvar, Complexities of assessing the disease burden attributable to leishmaniasis, PLoS Negl. Trop. Dis. 2 (10) (2008) e313.
[7] E. Schwartz, C. Hatz, J. Blum, New world cutaneous leishmaniasis in travellers, Lancet Infect. Dis. 6 (6) (2006) 342–349.
[8] S.D. Lawn, J. Whetham, P.L. Chiodini, J. Kanagalingam, J. Watson, R.H. Behrens, D.N. Lockwood, New world mucosal and cutaneous leishmaniasis: an emerging health problem among British travellers, QJM 97 (12) (2004) 781–788.
[9] D. Campbell-Lendrum, J.P. Dujardin, E. Martinez, M.D. Feliciangeli, J.E. Perez, L.N. Silans, P. Desjeux, Domestic and peridomestic transmission of American cutaneous leishmaniasis: changing epidemiological patterns present new control opportunities, Mem. Inst. Oswaldo Cruz 96 (2) (2001) 159–162.
[10] J.A. Patz, T.K. Graczyk, N. Geller, A.Y. Vittor, Effects of environmental change on emerging parasitic diseases, Int. J. Parasitol. 30 (12–13) (2000) 1395–1405.
[11] P. Desjeux, Leishmaniasis: current situation and new perspectives, Comp. Immunol. Microbiol. Infect. Dis. 27 (5) (2004) 305–318.
[12] J. Blum, P. Desjeux, E. Schwartz, B. Beck, C. Hatz, Treatment of cutaneous leishmaniasis among travellers, J. Antimicrob. Chemother. 53 (2) (2004) 158–166.
[13] R.D. Pearson, S.M.B. Jeronimo, A.Q. Sousa, in: S.H. Gillespie, R. D. Peason (Eds.), Principles and Practice of Clinical Parasitology, Vol. 1, John Wiley & Sons, Chichester, 2001, pp. 287–313.
[14] L. Sanchez-Saldana, Leishmaniasis, Dermatol. Peru 14 (2) (2004) 82–98.
[15] J. Ampuero Vela, Leishmaniasis, Ministerio de Salud, Lima, Peru, 2000.
[16] F. Modabber, P.A. Buffet, E. Torreele, G. Milon, S.L. Croft, Consultative meeting to develop a strategy for treatment of cutaneous leishmaniasis. Institute Pasteur, Paris. 13–15 June, 2006, Kinetoplastid Biol. Dis. 6 (2007) 3.
[17] P. Minodier, P. Parola, Cutaneous leishmaniasis treatment, Travel Med. Infect. Dis. 5 (3) (2007) 150–158.
[18] D. Vardy, Y. Barenholz, N. Naftoliev, S. Klaus, L. Gilead, S. Frankenburg, Efficacious topical treatment for human cutaneous leishmaniasis with ethanolic lipid amphotericin B, Trans. R. Soc. Trop. Med. Hyg. 95 (2) (2001) 184–186.
[19] A. Zvulunov, E. Cagnano, S. Frankenburg, Y. Barenholz, D. Vardy, Topical treatment of persistent cutaneous leishmaniasis with ethanolic lipid amphotericin B, Pediatr. Infect. Dis. J. 22 (6) (2003) 567–569.
[20] T. Hasan, B. Ortel, N. Solban, B. Pogue, in: D.W. Kufe, R.C.J Bast, W.N. Hait, W.K. Hong, R. Pollock, R.R. Weichselbaum, H.J. Gansler T, E. Frei III (Eds.), Cancer Medicine, BC Decker Inc., Hamilton, Ontario, Canada, 2006, pp. 537–548.
[21] Y. Nitzan, H.M. Wexler, S.M. Finegold, Inactivation of anaerobic bacteria by various photosensitized porphyrins or by hemin, Curr. Microbiol. 29 (3) (1994) 125–131.
[22] P.G. Calzavara-Pinton, M. Venturini, R. Sala, A comprehensive overview of photodynamic therapy in the treatment of superficial fungal infections of the skin, J. Photochem. Photobiol. B 78 (1) (2005) 1–6.
[23] S. Sohl, F. Kauer, U. Paasch, J.C. Simon, Photodynamic treatment of cutaneous leishmaniasis, J. Dtsch Dermatol. Ges. 5 (2) (2007) 128–130.
[24] K. Pizinger, P. Cetkovska, D. Kacerovska, M. Kumpova, Successful treatment of cutaneous leishmaniasis by photodynamic therapy and cryotherapy, Eur. J. Dermatol. 19 (2) (2009) 172–173.
[25] E.M. van der Snoek, D.J. Robinson, J.J. van Hellemond, H.A. Neumann, A review of photodynamic therapy in cutaneous leishmaniasis, J. Eur. Acad. Dermatol. Venereol. 22 (8) (2008) 918–922.
[26] N.I.H, NIH Clinical Trials ID: NCT00840359, Study of the Efficacy of Daylight Activated Photodynamic Therapy in the Treatment of Cutaneous Leishmaniasis, Hadassah Medical Organization, vol. 2009, 2009.
[27] J. Montanari, A.P. Perez, F. Di Salvo, V. Diz, R. Barnadas, L. Dicelio, F. Doctorovich, M.J. Morilla, E.L. Romero, Photodynamic ultradeformable liposomes: design and characterization, Int. J. Pharm. 330 (1–2) (2007) 183–194.
[28] C.J.F. Bötcher, C.M. Van Gent, C. Pries, A rapid and sensitive submicro phosphorus determination, Anal. Chim. Acta 24 (1961) 203–204.
[29] C. Korzeniewski, D.M. Callewaert, An enzyme-release assay for natural cytotoxicity, J. Immunol. Meth. 64 (3) (1983) 313–320.
[30] F. Tietze, Enzymic method for quantitative determination of nanogram amounts of total and oxidized glutathione: applications to mammalian blood and other tissues, Anal. Biochem. 27 (3) (1969) 502–522.
[31] B.C. Walton, J.J. Shaw, R. Lainson, Observations on the in vitro cultivation of Leishmania braziliensis, J. Parasitol. 63 (6) (1977) 1118–1119.
[32] S.M. Harrison, B.W. Barry, P.H. Dugard, Effects of freezing on human skin permeability, J. Pharm. Pharmacol. 36 (4) (1984) 261–262.
[33] U. Schaefer, H. Loth, An ex vivo model for the study of drug penetration into human skin, Pharm. Res. 13 (1996) 66.
[34] D.W. Fry, J.C. White, I.D. Goldman, Rapid separation of low molecular weight solutes from liposomes without dilution, Anal. Biochem. 90 (2) (1978) 809–815.
[35] H. Wagner, K.H. Kostka, C.M. Lehr, U.F. Schaefer, Drug distribution in human skin using two different in vitro test systems: comparison with in vivo data, Pharm. Res. 17 (12) (2000) 1475–1481.

[36] F.L. Primo, M.M.A. Rodrigues, A.R. Simioni, M.V.L.B. Bentley, P.C. Morais, A.C. Tedesco, In vitro studies of cutaneous retention of magnetic nanoemulsion loaded with zinc phthalocyanine for synergic use in skin cancer treatment, J. Magn. Magn. Mater. 320 (2008) e211–e214.
[37] K.A. Mullin, B.J. Foth, S.C. Ilgoutz, J.M. Callaghan, J.L. Zawadzki, G.I. McFadden, M.J. McConville, Regulated degradation of an endoplasmic reticulum membrane protein in a tubular lysosome in Leishmania mexicana, Mol. Biol. Cell 12 (8) (2001) 2364–2377.
[38] G. Cevc, A. Schatzlein, H. Richardsen, Ultradeformable lipid vesicles can penetrate the skin and other semi-permeable barriers unfragmented. Evidence from double label CLSM experiments and direct size measurements, Biochim. Biophys. Acta 1564 (1) (2002) 21–30.
[39] P.L. Honeywell-Nguyen, H.W. Wouter Groenink, A.M. de Graaff, J.A. Bouwstra, The in vivo transport of elastic vesicles into human skin: effects of occlusion, volume and duration of application, J. Control. Release 90 (2) (2003) 243–255.
[40] P.L. Honeywell-Nguyen, G.S. Gooris, J.A. Bouwstra, Quantitative assessment of the transport of elastic and rigid vesicle components and a model drug from these vesicle formulations into human skin in vivo, J. Invest. Dermatol. 123 (5) (2004) 902–910.
[41] A. Henning, U.F. Schaefer, D. Neumann, Potential pitfalls in skin permeation experiments: influence of experimental factors and subsequent data evaluation, Eur. J. Pharm. Biopharm. 72 (2) (2009) 324–331.
[42] J.-C. Tsai, M.J. Cappel, N.D. Weiner, G.L. Flynn, J.J. Ferry, Solvent effects on the harvesting of stratum corneum from hairless mouse skin through adhesive tape stripping in vitro, Int. J. Pharm. 68 (1–3) (1991) 127–133.
[43] B.A. van den Bergh, J.A. Bouwstra, H.E. Junginger, P.W. Wertz, Elasticity of vesicles affects hairless mouse skin structure and permeability, J. Control. Release 62 (3) (1999) 367–379.
[44] P.L. Honeywell-Nguyen, A.M. de Graaff, H.W. Groenink, J.A. Bouwstra, The in vivo and in vitro interactions of elastic and rigid vesicles with human skin, Biochim. Biophys. Acta 1573 (2) (2002) 130–140.
[45] K.A. Holbrook, G.F. Odland, Regional differences in the thickness (cell layers) of the human stratum corneum: an ultrastructural analysis, J. Invest. Dermatol. 62 (4) (1974) 415–422.
[46] G. Cevc, G. Blume, Lipid vesicles penetrate into intact skin owing to the transdermal osmotic gradients and hydration force, Biochim. Biophys. Acta 1104 (1) (1992) 226–232.
[47] J.P. Ryman-Rasmussen, J.E. Riviere, N.A. Monteiro-Riviere, Penetration of intact skin by quantum dots with diverse physicochemical properties, Toxicol. Sci. 91 (1) (2006) 159–165.
[48] O.E. Akilov, S. Kosaka, K. O'Riordan, T. Hasan, Parasiticidal effect of delta-aminolevulinic acid-based photodynamic therapy for cutaneous leishmaniasis is indirect and mediated through the killing of the host cells, Exp. Dermatol. 16 (8) (2007) 651–660.
[49] C.D. Enk, C. Fritsch, F. Jonas, A. Nasereddin, A. Ingber, C.L. Jaffe, T. Ruzicka, Treatment of cutaneous leishmaniasis with photodynamic therapy, Arch. Dermatol. 139 (4) (2003) 432–434.
[50] K. Gardlo, S. Hanneken, T. Ruzicka, N.J. Neumann, Photodynamic therapy of cutaneous leishmaniasis. A promising new therapeutic modality, Hautarzt 55 (4) (2004) 381–383.
[51] K. Gardlo, Z. Horska, C.D. Enk, L. Rauch, M. Megahed, T. Ruzicka, C. Fritsch, Treatment of cutaneous leishmaniasis by photodynamic therapy, J. Am. Acad. Dermatol. 48 (6) (2003) 893–896.
[52] A. Asilian, M. Davami, Comparison between the efficacy of photodynamic therapy and topical paromomycin in the treatment of Old World cutaneous leishmaniasis: a placebo-controlled, randomized clinical trial, Clin. Exp. Dermatol. 31 (5) (2006) 634–637.
[53] O.E. Akilov, S. Kosaka, K. O'Riordan, T. Hasan, Photodynamic therapy for cutaneous leishmaniasis: the effectiveness of topical phenothiaziniums in parasite eradication and Th1 immune response stimulation, Photochem. Photobiol. Sci. 6 (10) (2007) 1067–1075.
[54] P. Escobar, I.P. Hernandez, C.M. Rueda, F. Martinez, E. Paez, Photodynamic activity of aluminium (III) and zinc (II) phthalocyanines in Leishmania promastigotes, Biomedical 26 (Suppl 1) (2006) 49–56.
[55] S. Dutta, D. Ray, B.K. Kolli, K.P. Chang, Photodynamic sensitization of Leishmania amazonensis in both extracellular and intracellular stages with aluminum phthalocyanine chloride for photolysis in vitro, Antimicrob. Agents Chemother. 49 (11) (2005) 4474–4484.
[56] J. Moan, K. Berg, The photodegradation of porphyrins in cells can be used to estimate the lifetime of singlet oxyge, Photochem. Photobiol. 53 (4) (2001) 549–553.
[57] A.P. Castano, T. Demidova, M.R. Hamblin, Mechanisms in photodynamic therapy: part one—photosensitizers, photochemistry and cellular localization, Photodiagn. Photodyn. Ther. 1 (4) (2004) 279–293.
[58] C.A. Robertson, D.H. Evans, H. Abrahamse, Photodynamic therapy (PDT): a short review on cellular mechanisms and cancer research applications for PDT, J. Photochem. Photobiol. B 96 (1) (2009) 1–8.
[59] A. Ketabchi, A. MacRobert, P.M. Speight, J.H. Bennett, Induction of apoptotic cell death by photodynamic therapy in human keratinocytes, Arch. Oral Biol. 43 (2) (1998) 143–149.
[60] S. Coppola, L. Ghibelli, GSH extrusion and the mitochondrial pathway of apoptotic signalling, Biochem. Soc. Trans. 28 (2) (2000) 56–61.
[61] R.M. Steinman, I.S. Mellman, W.A. Muller, Z.A. Cohn, Endocytosis and the recycling of plasma membrane, J. Cell Biol. 96 (1) (1983) 1–27.
[62] A. Papagiannaros, C. Bories, C. Demetzos, P.M. Loiseau, Antileishmanial and trypanocidal activities of new miltefosine liposomal formulations, Biomed. Pharmacother. 59 (10) (2005) 545–550.
[63] P. Overath, Y.D. Stierhof, M. Wiese, Endocytosis and secretion in trypanosomatid parasites — Tumultuous traffic in a pocket, Trends Cell Biol. 7 (1) (1997) 27–33.
[64] S.M. Landfear, M. Ignatushchenko, The flagellum and flagellar pocket of trypanosomatids, Mol. Biochem. Parasitol. 115 (1) (2001) 1–17.
[65] G. Cevc, in: Lipowsky, Sachman (Eds.), Handbook of Biological Physics, Vol. I, Elsevier Science BV, Amsterdam, 1995, pp. 465–489.
[66] P.L. Honeywell-Nguyen, J.A. Bouwstra, Vesicles as a tool for transdermal and dermal delivery, Drug Discov. Today: Technol. 2 (1) (2005) 67–74.
[67] J.A. Cowen, R.E. Imhof, P. Xiao, Opto-thermal measurement of stratum corneum renewal time, Anal. Sci. 17 (2001) s353–s356.
[68] J.P. Ryman-Rasmussen, J.E. Riviere, N.A. Monteiro-Riviere, Variables influencing interactions of untargeted quantum dot nanoparticles with skin cells and identification of biochemical modulators, Nano Lett. 7 (5) (2007) 1344–1348.